Topological Relations between Discrete Regions

Stephan Winter*
Institute for Photogrammetry, University of Bonn, Germany

In: Advances of Spatial Databases, Proc. Fourth Symposium on Large Spatial Databases (SSD '95), Portland, Maine. Springer, LNCS 951, pp. 310-328

Abstract

Topological reasoning is important for speeding up spatial queries, e.g. in GIS or in AI (robotics). While topological relations between spatial objects in the vector model ($\mathbb{R}^2$) are investigated thoroughly, we run into inconsistencies in the raster model ($\mathbb{Z}^2$). But instead of reducing our requirements in case of reasoning in raster images we change from simple raster to a cellular decomposition of $\mathbb{R}^2$ — what we call a hyper-raster — which is also discrete, but preserves the topology of $\mathbb{R}^2$. The discrete representation reduces the computational effort against the vector model.

We will introduce a data structure for the hyper-raster, which represents regions, curves and points. Then we will present algorithms for digitization (vector/hyper-raster conversion). With the hyper-raster the intersection sets, as needed for the determination of a topological relation between two objects, are calculated simply by logical joins of binary images. Without extending our model we can also compute further refinements of the relationships.

1 Introduction

Topological relations have been found useful for speeding up spatial queries, e.g. in GIS or in AI (robotics). The analysis of topological relations may reduce the burden of geometric computations. Sometimes they are solely sufficient, and no further geometric analysis is needed. Therefore, topology should be taken into consideration in spatial data modeling.

While topological relations between spatial objects in the vector model ($\mathbb{R}^2$) can be based on Euclidean topology, which has lead to a symbolic reasoning framework (e.g. Egenhofer and Franzosa 1991, Egenhofer and Herring 1991, Clementini and Di Felice 1994), the '*digital topology*' of the raster model ($\mathbb{Z}^2$, Kong and Rosenfeld 1989, Latecki 1992) is not as powerful and needs conceptual extensions of the cited framework (Egenhofer and Sharma 1993). Instead of reducing our requirements in case of reasoning in raster images we propose to change from simple raster to a cellular decomposition of $\mathbb{R}^2$ (Kovalevski 1989) — what we call a hyper-raster —, which is also discrete, but preserves the topology of $\mathbb{R}^2$.

- We show that the hyper-raster is an intuitive and convenient model to describe topological properties and relations, contrary to the raster. We demonstrate the suitability for topological reasoning by applying Egenhofer's framework of 9-intersections (Egenhofer and Franzosa 1991), without any contradiction or conceptual difference to the vector model.
- The finiteness of the decomposition, in combination with a separate storage of hyper-raster element types, allows to applicate image processing algorithms (Kovalevski 1989, Bieri and Metz 1991). This will speed up the reasoning. We show in a practical example how to apply the reasoning framework to the hyper-raster.

*Supported by the *Deutsche Forschungsgemeinschaft*, Sonderforschungsbereich 350.

In this paper we concentrate on relations between regions without holes. This is taken as an example, because the hyper-raster is neither limited in representing spatial objects of other dimensions, or holes, nor in topological properties. Both are pointed out in the corresponding sections. Also taking into consideration holes, or lines and points, would only cause additional complexity in reasoning, and would take away the intuitive clarity of this short paper.

This paper has the following structure. After an overview of the relevant notions of topology we summarize the work of others in topological reasoning. Then we introduce the hyper-raster model and a proper data structure for the representation of regions, curves and points. We will also describe the vector-to-hyper-raster conversion. After transferring the 9-intersection to the hyper-raster we specify the calculation of the 9-intersection. The calculation is reduced to logical joins of binary images. Without model extensions we can also compute further refinements of the relationship by image analysis, e.g. the number, the size, the dimension or the shape of intersection components.

An example will demonstrate the operability. The properties of the hyper-raster recommend it as a possible component to integrate vector-based and raster-based spatial data models.

2 Topological Models for GIS

In this chapter we give a short summary of the notions of *algebraic* and *digital topology*, pointing out the conceptional difference of vector and raster. Furthermore we introduce the hyper-raster as a regular cellular complex.

2.1 Euclidean Topology

In $\mathbb{R}^2$ we refer to Euclidean topology. Euclidean space is a topological space, that means (Jänich 1994):

Definition 2.1: A *topological space* is a pair $(X, \mathcal{O})$ of a set X and a set $\mathcal{O}$ of subsets of X, called the open sets, which satisfy

1. the union of open sets is open,
2. the intersection of finitely many open sets is open,
3. $\emptyset$ and X are open.

To become a metric space, a distance measure d has to be introduced additionally. Confining here to Euclidean topology, the Euclidean distance is chosen.

Definition 2.2: If (X, d) is a metric space, then a subset $V \subset X$ is called *open*, if for all $x \in V$ an $\varepsilon > 0$ exists with the sphere $K_\varepsilon(x) := \{y \in X | d(x, y) \leq \varepsilon\}$ in V. The set $\mathcal{O}(d)$ of all open subsets of X is called the *topology of the metric space* (X, d).

The topology of $\mathbb{R}^2$ is used widely in *data modeling* (e.g. Herring 1987, Bennis *et al.* 1991, Pigot 1991, Molenaar *et al.* 1994, Pilouk *et al.* 1994), and also in *topological reasoning* (Egenhofer and Franzosa 1991, Clementini and Di Felice 1994, and Hernández 1994).

In $\mathbb{R}^2$ Jordan's curve theorem is valid, which is important in the following sections:

Theorem 2.1: A simple closed and continuous curve divides the plane into two regions, the interior and the exterior.

2.2 Digital Topology

This short summary of topological deficiencies of raster images is to contrast with the hyper-raster, which is based on Euclidean topology. The hyper-raster follows in the next section.

A raster is a two-dimensional array of elements with integer coordinates, which can also be interpreted as a lattice $\mathbb{Z} \times \mathbb{Z}$. The raster is only of trivial topology, because the definition of a distance notion is possible, but all sets in a raster are open. Mathematicians speak of *digital topology*, but we have to pay attention to the different meaning of the notion in image processing literature.

Because in a raster we can not distinguish between open and closed sets, the difference between the closure of a pixel set and the open interior is empty, so we have no boundary in a raster. Also Jordan's curve theorem is only applicable with additional definitions of a neighborhood and a boundary curve (Kong and Rosenfeld 1989).

The '*digital topology*', as surveyed by Kong and Rosenfeld (1989) for the use in binary image analysis, differs from the above mentioned topology, because it does not refer to the definition of a topological space. To avoid paradoxa, all topological notions were defined algorithmically, and not by a derivation from the definitions of Sect. 2.1.

However, Kong and Rosenfeld discuss topological properties of binary image arrays. An interior (resp. exterior) boundary curve is introduced as a sequence of interior (resp. exterior) border points. These substitutes for boundary curves have a certain extent. Topologically they are 2D-sets, i.e. regions. Only with different concepts of pixel neighborhood for foreground and background is Jordan's curve theorem valid in the raster model. But these definitions cause contradictions if we permute foreground and background. Latecki *et al.* (1995) limit the raster model by excluding the pixel compositions which cause paradoxical interpretations, thus foreground-background contradictions will not occur. However, in this limited model, curves have to be defined as two-dimensional structures.

This '*digital topology*' of Kong and Rosenfeld, further restricted by some conditions concerning the size and shape of regions, is used by Egenhofer and Sharma (1993), as referred in Section 3.2. They have to model the results of the topological deficiencies, while our proposal to use the hyper-raster instead does not leave Euclidean topology.

2.3 Cellular Decomposition

We are now prepared to introduce the hyper-raster. Using notions from the Euclidean topology (Sect. 2.1) we define (Jänich 1994):

Definition 2.3: We call a topological space an *n-cell*, if it is homeomorphic to $\mathbb{R}^n$.

A *cellular decomposition* $(X, \mathcal{E})$ of a topological space X is a decomposition of X into parts $\mathcal{E}$, which are cells by themselves.

We distinguish further:

Definition 2.4: The *interior* of a region $\mathcal{R}$, $\overset{\circ}{\mathcal{R}}$, is a connected and open complex of dimension 2.

The *closure* of a region $\mathcal{R}$, $\overline{\mathcal{R}}$, is the minimal sub-complex which contains the interior of $\mathcal{R}$ and all faces of the elements of $\overset{\circ}{\mathcal{R}}$.

The *boundary* of a region $\mathcal{R}$, $\partial\mathcal{R}$, is now $\partial\mathcal{R} = \overline{\mathcal{R}} \setminus \overset{\circ}{\mathcal{R}}$.

The *complement* $\mathcal{R}^c$ of a region $\mathcal{R}$ is $\mathcal{R}^c = X \setminus \overline{\mathcal{R}}$.

It follows that the boundary of a region is at the same time the boundary of its complement.

For example, the *vector model* of spatial databases is based on an irregular cellular decomposition of a surface (2.5D) or a plane (2D). In the vector model boundaries of regions are represented as closed polygons. Polygons are continuous curves by nature, because the line segments are connected by common vertices. Therefore, Jordan's curve theorem (Theorem 2.1) is valid for the vector model.

To overcome the topological problems with $\mathbb{Z}^2$, Kovalevski (1989) proposes a *regular* cellular decomposition of the plane. This decomposition only limits the set of considered structures in $\mathbb{R}^2$ to regular shaped cells, but it preserves the topology of $\mathbb{R}^2$, as the decomposition is embedded in the continuous plane (homeomorphism). This decomposition is able to substitute the image model[1] of $\mathbb{Z}^2$ (raster).

To decompose the plane, we choose axis-parallel, open quadrangles of the side length 1 as 2-cells. 1-cells are faces of 2-cells, and 0-cells are faces of 1-cells (Fig. 1), the empty cell is admitted also. In this cellular complex a *curve* is a connected chain of 1D- and 0D-cells.

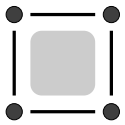

Figure 1: A cell complex, replacing one pixel.

Kovalevski (1989) picks up the cellular decomposition for the use in image analysis, proposing a cell list data structure and algorithms for image encoding, and Bieri and Metz (1991) apply a tree structure for storing cellular decomposed binary images.

In the remainder of this paper we will call the regular cellular complex a *hyper-raster*, according to Bieri and Metz. Also we will present an own data structure, which is to demonstrate the applicability of topological reasoning more intuitively.

3 Topological Reasoning in GIS

The main use of topological reasoning in spatial databases is to analyze topological relationships before extensive geometric computations. A symbolic reasoning method for the vector model, based on the topology of cell complexes, has been built up by Egenhofer and Franzosa (1991) and Egenhofer and Herring (1991), which we will summarize shortly.

3.1 The 9-Intersection Model in $\mathbb{R}^2$

Egenhofer and Franzosa proposed a method of representing topological relationships by calculating the four intersection sets of the interior and the boundary of two regions without holes, i.e. regions with connected boundaries (*4-intersection model*). They found eight unique and mutually exclusive relations. Egenhofer and Herring expanded the model to a *9-intersection*, also taking into consideration the exterior of regions $\mathcal{R}$, $\mathcal{R}^c$. The 9-intersection can be denoted by a matrix $\mathbf{I}_{33}$:

$$\mathbf{I}_{33} = \begin{pmatrix} \mathring{\mathcal{A}} \cap \mathring{\mathcal{B}} & \mathring{\mathcal{A}} \cap \partial\mathcal{B} & \mathring{\mathcal{A}} \cap \mathcal{B}^c \\ \partial\mathcal{A} \cap \mathring{\mathcal{B}} & \partial\mathcal{A} \cap \partial\mathcal{B} & \partial\mathcal{A} \cap \mathcal{B}^c \\ \mathcal{A}^c \cap \mathring{\mathcal{B}} & \mathcal{A}^c \cap \partial\mathcal{B} & \mathcal{A}^c \cap \mathcal{B}^c \end{pmatrix} \tag{1}$$

[1] 1D-edge elements between raster pixels have already been used in image segmentation, there better known as *crack edges* (see e.g. Ballard and Brown 1982, Bässmann and Besslich 1991.

The five additional intersection sets of the $\mathbf{I}_{33}$ also allow to handle relations between regions with holes and relations between regions, lines and points (cf. Table 1). However, they do not allow to refine the eight relations of regions with more details (cf. Table 2), as it is done by other indicators (Sect. 3.3).

Table 1: Number of real relations between spatial objects (taken from Egenhofer and Herring (1991)). The first item refers to simple objects, the second item (bracketed) to complex objects (complex region: region with holes; complex line: line with more than two boundary points).

Relation between ...	region	line	point
region	8 (18)	19 (20)	3
line		33 (57)	3
point			2

Table 2: The eight topologic relations between two regions without holes, associated with the 9-intersection $\mathbf{I}_{33}$.

$$\begin{pmatrix} \emptyset & \emptyset & \neg\emptyset \\ \emptyset & \emptyset & \neg\emptyset \\ \neg\emptyset & \neg\emptyset & \neg\emptyset \end{pmatrix}$$ DISJOINT

$$\begin{pmatrix} \emptyset & \emptyset & \neg\emptyset \\ \emptyset & \neg\emptyset & \neg\emptyset \\ \neg\emptyset & \neg\emptyset & \neg\emptyset \end{pmatrix}$$ MEETS

$$\begin{pmatrix} \neg\emptyset & \neg\emptyset & \neg\emptyset \\ \neg\emptyset & \neg\emptyset & \neg\emptyset \\ \neg\emptyset & \neg\emptyset & \neg\emptyset \end{pmatrix}$$ OVERLAPS

$$\begin{pmatrix} \neg\emptyset & \emptyset & \emptyset \\ \emptyset & \neg\emptyset & \emptyset \\ \emptyset & \emptyset & \neg\emptyset \end{pmatrix}$$ EQUALS

$$\begin{pmatrix} \neg\emptyset & \neg\emptyset & \neg\emptyset \\ \emptyset & \neg\emptyset & \neg\emptyset \\ \emptyset & \emptyset & \neg\emptyset \end{pmatrix}$$ COVERS

$$\begin{pmatrix} \neg\emptyset & \emptyset & \emptyset \\ \neg\emptyset & \neg\emptyset & \emptyset \\ \neg\emptyset & \neg\emptyset & \neg\emptyset \end{pmatrix}$$ COVEREDBY

$$\begin{pmatrix} \neg\emptyset & \neg\emptyset & \neg\emptyset \\ \emptyset & \emptyset & \neg\emptyset \\ \emptyset & \emptyset & \neg\emptyset \end{pmatrix}$$ CONTAINS

$$\begin{pmatrix} \neg\emptyset & \emptyset & \emptyset \\ \neg\emptyset & \emptyset & \emptyset \\ \neg\emptyset & \neg\emptyset & \neg\emptyset \end{pmatrix}$$ CONTAINEDBY

Referring to the complex calculation of the additional sets — the exterior of the treated regions is much larger, or goes to infinity, compared to the size of the treated regions themselves — Egenhofer and Herring propose a combination of the 4-intersection and additional criterion to resolve ambiguities in the extended analyses. Egenhofer *et al.* (1994a), who are also interested on regions with holes, solve ambiguities by reasoning about generalized regions, neglecting the holes. But as we will see, the complexity of calculation with the exterior of spatial objects can be eliminated (Sect. 4.4).

In this paper we confine ourselves to regions without holes. The hyper-raster would also work with objects of other dimensions, or with regions with holes, in full accordance to the vector model. However, we prefer a clearly arranged example for topological reasoning, having only eight distinct relations. Another reason is the reference to the work of Egenhofer and Sharma (1993), who adapted the 9-intersection to the raster, for regions without holes. In principle, in the hyper-raster the 4-intersection would be sufficient for representing the expected eight relations. But due to comparability to the raster we will draw up the 9-intersection in the following. Should we ever want to extend the reasoning in hyper-raster we would have to use the 9-intersection in any case.

3.2 The 9-Intersection Model in $\mathbb{Z}^2$

Egenhofer and Sharma (1993) applied the 9-intersection to raster regions, using a 4-adjacency and the interior boundary (which has a diameter of one pixel), in concordance with the '*digital topology*' (Sect. 2.2). Constraints about consistent combinations in the 9-intersection reduce the number of possible relations from $2^9 = 512$ to 16, all with a geometric interpretation. These relations can be ordered in a conceptual-neighborhood-graph, which has clusters comparable to the relations of $\mathbb{R}^2$.

The number of relations differs from those which occur in $\mathbb{R}^2$. The first reason is the two-dimensional boundary, which allows intersection sets that would be inconsistent in $\mathbb{R}^2$. The second reason is the conceptual deficiency in the limitation to interior boundaries, which leads Egenhofer and Sharma to the interpretation that topology in the discrete space is based not only on coincidence of boundaries but also on neighbored boundaries. This is a problematic point of view, because it is more the deficiency of '*digital topology*' than of discretisation, as we will show for the hyper-raster.

3.3 Refinements of Topological Reasoning

The literature presented some ideas which described topological relations more detailed as by a binary $\mathbf{I}_{33}$. We will pick up them for reasoning in the hyper-raster.

One refinement of modeling topological relationships was the idea of replacing the binary intersection matrix by a matrix indicating the dimension of an intersection set: -1D (for $\emptyset$), 0D, 1D, or 2D, cf. Table 3 (Clementini *et al.* 1993).

Table 3: The possible dimension of intersection sets.

	$\mathring{\mathcal{B}}$	$\partial\mathcal{B}$	$\mathcal{B}^c$
$\mathring{\mathcal{A}}$	$\{-1D \vee 2D\}$	$\{-1D \vee 1D\}$	$\{-1D \vee 2D\}$
$\partial\mathcal{A}$	$\{-1D \vee 1D\}$	$\{-1D \vee 0D \vee 1D\}$	$\{-1D \vee 1D\}$
$\mathcal{A}^c$	$\{-1D \vee 2D\}$	$\{-1D \vee 1D\}$	$\{-1D \vee 2D\}$

Egenhofer (1993) also specifies topological relations in a more detailed way, by additional numerical topological invariants: the dimension of intersections, and the number of components of an intersection set. Other topological invariants are added in a multiple representation framework in Egenhofer *et al.* (1994b).

4 The Hyper-Raster Model

Now we propose to applicate the cellular decomposition of $\mathbb{R}^2$ (cf. Sect. 2.3) as a data model for digital images. We develop here a data structure for the hyper-raster, which we will use later for topological reasoning (Sect. 4.4).

A sketch of the hyper-raster shows 2D picture elements, enriched by edge and node elements (Fig. 2). While the hyper-raster consists of elements with different dimensions, behavior and meaning, a data structure for the hyper-raster should be able to distinguish between the element types, too. The data structure should also be able to handle all spatial entities of the plane: points, curves and regions. Furthermore we want to preserve the two-dimensional array structure to apply image processing algorithms later.

Therefore, we now introduce a class *hyperimage*, which consists of separate matrices for the element types, and of methods to handle the interrelation of the matrices and to adopt image processing algorithms.

4.1 Hyperimage: a Hyper-Raster Data Structure

Data elements of the class *hyperimage* are a matrix **C** for the 2D-cells, a matrix **E** for the horizontal and vertical edge elements, and a matrix **N** for the vertices. A cell decomposition of an area of

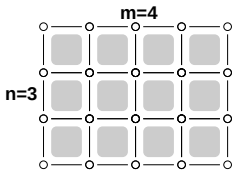

Figure 2: The hyper-raster with separable element types: picture elements, edges and vertices.

size $n * m$ will lead to $n * m$ 2D-cells, $(n + 1) * m$ horizontal edges, $n * (m + 1)$ vertical edges, and $(n + 1) * (m + 1)$ vertices[2] (cf. Fig. 2).

Storing vertical edges and horizontal edges separately, e.g. in matrices $\mathbf{V}$ and $\mathbf{H}$, has some disadvantages[3]. But the unique matrix $\mathbf{E}$ we introduced instead of $\mathbf{V}$ and $\mathbf{H}$ maintains the connectedness of the boundary, by 8-adjacency. $\mathbf{E}$ is built by resampling the hyper-raster into a matrix rotated by 45° and scaled by $\sqrt{2}$. Then each edge element is associated with one rotated pixel (Fig. 3, cf. also Fig. 6) (Kropatsch 1985, Kropatsch 1986).

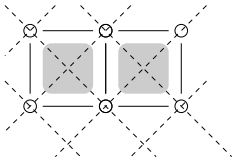

Figure 3: A rotated matrix can store all edge elements.

While the size of $\mathbf{H}$ and $\mathbf{V}$ is together $2nm+n+m$, the size of $\mathbf{E}$ is $(n+m)^2 = 2nm+n^2+m^2$. So, if memory becomes a problem, the implemented data model should be changed, e.g. to a list structure.

Separating the hyper-raster elements requires access methods (rules) to identify the faces of a single element of $\mathbf{C}$, $c_{i,j}$, and vice versa. The four vertices of a picture element $c_{i,j}$ are found at $n_{i,j}$ (north-west), $n_{i+1,j}$ (south-west), $n_{i+1,j+1}$ (south-east), and $n_{i,j+1}$ (north-east). The upper edge of $c_{i,j}$ is found at $e_{i+j,\text{rows}-i+j}$, the left edge is found at $e_{i+j,\text{rows}-i+j-1}$, and so on. The access rules are part of the data encapsulation.

With this set of three separate matrices we have to model two different tasks:

- to represent the spatial entities (point, curve, region), we introduce a set of *labeling* matrices $\mathbf{C}_l$, $\mathbf{E}_l$, and $\mathbf{N}_l$. $\mathbf{C}_l$ contains region labels, with the condition that one pixel may only belong to one label class, $\mathbf{E}_l$ contains curve labels, and $\mathbf{N}_l$ point labels, both with the same condition.

  Because in this paper we concentrate on regions (without holes), in the remainder we only refer to $\mathbf{C}_l$.

- to represent the boundaries of spatial entities, we introduce *boundary* matrices $\mathbf{C}_b$, $\mathbf{E}_b$, and $\mathbf{N}_b$. Because 2-cells are boundaries of volumes — which we exclude —, we can remove $\mathbf{C}_b$ from this set. Then $\mathbf{E}_b$ contains the arcs of the boundaries of regions, and $\mathbf{N}_b$ contains both, the vertices of the boundaries of regions, and the bounding vertices of curves. Storing a point's boundary is not necessary because it coincides with the point.

  Also here the context of this paper allows us to confine ourselves to *region boundaries* in $\mathbf{E}_b$ and $\mathbf{N}_b$.

[2] On the other hand Bieri and Metz (1991) propose to normalize the hyper-raster, which yields other numbers.

[3] For example, a boundary of a rectangle splits in $\mathbf{H}$ into two components, the upper and the lower boundary, and in $\mathbf{V}$ into the left and the right boundary. This is undesired in some applications, like contour detection.

The elementary data type of the labeling matrices depends on the maximum number of spatial objects (# labels), while the type of the boundary matrices depends on the amount of information we wish to store. In the simplest case binary matrices — (*boundary element, not boundary element*) — are sufficient.

4.2 Digitization

To convert a vector data set into a hyper-raster, the digitization rules are slightly different from those for the raster, with regard to curves and points. Digitizing a point means labeling the nearest 0-cell in $\mathbf{N}_l$. Digitizing a curve requires to label a closed chain of 1-cells (in $\mathbf{E}_l$) between start and end vertex (in $\mathbf{N}_b$). A region will be digitized by converting the boundary, a closed polygon, into $\mathbf{E}_b$ and $\mathbf{N}_b$, and afterwards labeling the interior in $\mathbf{C}_l$. Some attention has to be paid to avoid degenerated regions. A degeneration consists of 1-cells in the boundary (and, because of redundancy, also of 0-cells) which have no 2-cell labeled as interior. This can occur, if the resolution of the discretisation is not sufficient (cf. Fig. 4).

The digitization rules are implemented as a part of the constructor of a hyperimage. If a vector data set of regions is digitized, the result is a fully segmented and classified matrix $\mathbf{C}_l$, and binary matrices $\mathbf{E}_b$ and $\mathbf{N}_b$. With regard to topological reasoning, the matrices $\mathbf{E}_b$ and $\mathbf{N}_b$, although redundant to a large degree, are both are necessary (cf. Table 4).

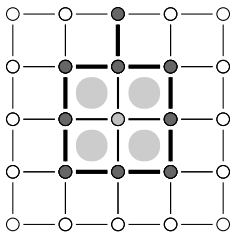

Figure 4: Degenerated region: a 1-cell of the boundary with no interior neighbor cells.

A topological relation is a binary relation, i.e. a relation between two spatial objects. Therefore, it is sufficient to digitize the two regions in question (if we start with vector data sets), or to extract single regions (if we start with hyper-raster maps). Such a set of (binary) *extract matrices* $\mathbf{C}_e$, $\mathbf{E}_e$, and $\mathbf{N}_e$, build for each of both regions, can be limited in size to a bounding rectangle of the region. In $\mathbf{C}_e$ the interior of the region is foreground, and the exterior of the region is background, and in $\mathbf{E}_e$ and $\mathbf{N}_e$ the boundary of the region is foreground.

Our presented data structure is now complete for topological reasoning. The next step is to transfer the 9-intersection to the hyper-raster and then to apply it in the *hyperimage*.

4.3 The 9-Intersection in the Hyper-Raster

In the hyper-raster, we find exactly the eight relationships between regions which exist in $\mathbb{R}^2$. Egenhofer and Sharma (1993) cite five conditions to select the relations which really occur in $\mathbb{R}^2$ from the 512 possible states of the 9-intersection. In raster they may apply the first three conditions (which leads to remaining 16 relations), but here also the latter two conditions can be applied (leaving the known eight relations):

Condition 4.1: (4) If the interior of $\mathcal{A}$ intersects with the boundary of $\mathcal{B}$ then it must also intersect with the exterior of $\mathcal{B}$, and vice versa.

Condition 4.2: (5) If both interiors are disjoint then the boundary of $\mathcal{A}$ cannot intersect with the interior of $\mathcal{B}$, and vice versa.

Proof: Condition 4 follows from the hyper-raster property that intersections with boundary elements can only exist of 1D- or 0D-cells. But if an 1D-cell (and the more a 0D-cell) belongs to the interior of $\mathcal{A}$, then both neighbored 2D-cells belong to $\mathcal{A}$, too. Compared to it an 1D-cell of the boundary of $\mathcal{B}$ inevitably neighbors with one 2D-cell of the interior of $\mathcal{B}$ and one 2D-cell of the exterior of $\mathcal{B}$. Therefore, an intersection of the interior of $\mathcal{A}$ with the boundary of $\mathcal{B}$ implies that at least one neighbored 2D-cell of the boundary must fall on the exterior of $\mathcal{B}$, and one on the interior of $\mathcal{B}$. □ ■

Proof: Condition 5 rests upon the same hyper-raster property. An 1D-cell of the boundary of $\mathcal{A}$, and more an 0D-cell, inevitably neighbors with one 2D-cell of the interior of $\mathcal{A}$, and one 2D-cell of the exterior of $\mathcal{A}$. If the boundary of $\mathcal{A}$ intersects with the interior of $\mathcal{B}$, then at least one 2D-cell of the interior of $\mathcal{A}$ intersects with a 2D-cell of the interior of $\mathcal{B}$. □ ■

In principle, conditions from the vector model to exclude inconsistent combinations of the 9-intersection hold true for the hyper-raster analogously. That is because of the common spatial model of cellular decomposition. A confinement to regular cells is invariant to topological modeling. With that we may expect, that topological relations between spatial objects of other dimensions, or between regions with holes, will coincide to the vector model, too.

4.4 The 9-Intersection in the *Hyperimage*

With the *hyperimage* the 9-intersection is very fast to compute, contrary to the situation in the vector model. We have only to overlay the extracted object matrices (taking care of their different origin). The overlay is done by joining them with a logical '$\wedge$' pixel by pixel (this is equivalent to $\cap$ in set denotation). Then the foreground of the overlay represents an intersection set, or a part of it. As one property of the '$\wedge$'-operator the overlay can be limited to the overlap of the bounding rectangles of the considered regions.

Now we show how to enlarge the binary extracted matrices into three-valued matrices[4], specifying the *interior*, *boundary*, and *exterior* of a region $\mathcal{R}$. For simplicity we omit the index e of the extraction matrices in the following, and the foreground pixels of a matrix we denote by '$\mathcal{F}$'.

$$\begin{array}{lcl} \mathbf{C}(\mathring{\mathcal{R}}) & = & \bigcup c_{i,j} \mid c_{i,j} \in \mathcal{F} \\ \mathbf{C}(\partial\mathcal{R}) & = & \emptyset \\ \mathbf{C}(\mathcal{R}^c) & = & \bigcup c_{i,j} \mid c_{i,j} \notin \mathcal{F} = \bigcup c_{i,j} \setminus \{\mathbf{C}(\mathring{\mathcal{R}})\} \end{array} \tag{2}$$

$\mathbf{C}_e$ contains no boundary information and is really binary, therefore.

$$\begin{array}{lcl} \mathbf{E}(\mathring{\mathcal{R}}) & = & \bigcup e_{i,j} \mid (e_{i,j} \notin \mathcal{F}) \wedge (\sum(e_{k,j} \in \mathcal{F}) = \text{odd}), \text{ with } k = 0 \ldots i-1 \\ \mathbf{E}(\partial\mathcal{R}) & = & \bigcup e_{i,j} \mid e_{i,j} \in \mathcal{F} \\ \mathbf{E}(\mathcal{R}^c) & = & \bigcup e_{i,j} \mid (e_{i,j} \notin \mathcal{F}) \wedge (\sum(e_{k,j} \in \mathcal{F}) = \text{even}), \text{ with } k = 0 \ldots i-1 \\ & = & \bigcup(e_{i,j} \setminus \{\mathbf{E}(\mathring{\mathcal{R}}), \mathbf{E}(\partial\mathcal{R})\} \end{array} \tag{3}$$

Since $\mathbf{E}_e$ contains no degenerated elements (cf. Sect. 4.2), an element $e_{i,j}$ belongs to the interior of a region, if it is not boundary and if an odd number of boundary elements precede in the row i.

Also, $e_{i,j}$ is interior if it is not boundary, and if at least one neighbored 2-cell belongs to the foreground (interior).

[4] An alternative way is directly to extract ternary matrices (*interior, boundary, exterior*), but we are interested in the binary matrices for further processing.

To determine $\mathbf{N}(\overset{\circ}{\mathcal{R}})$, we have to check for each $n_{i,j}$ if it is not boundary, and if at least one neighbored 2-cell belongs to the foreground (interior).

$$\begin{array}{lcl} \mathbf{N}(\partial\mathcal{R}) & = & \bigcup n_{i,j} \mid n_{i,j} \in \mathcal{F} \\ \mathbf{N}(\mathcal{R}^c) & = & \bigcup n_{i,j} \setminus \{\mathbf{N}(\overset{\circ}{\mathcal{R}}), \mathbf{N}(\partial\mathcal{R})\} \end{array} \tag{4}$$

With that we can denote the three topological sets of a region $\mathcal{R}$ which occur in $\mathbf{I}_{33}$ as:

$$\begin{array}{lcl} \overset{\circ}{\mathcal{R}} & = & \mathbf{C}(\overset{\circ}{\mathcal{R}}) \cup \mathbf{E}(\overset{\circ}{\mathcal{R}}) \cup \mathbf{N}(\overset{\circ}{\mathcal{R}}) \\ \partial\mathcal{R} & = & \mathbf{C}(\partial\mathcal{R}) \cup \mathbf{E}(\partial\mathcal{R}) \cup \mathbf{N}(\partial\mathcal{R}) \\ \mathcal{R}^c & = & \mathbf{C}(\mathcal{R}^c) \cup \mathbf{E}(\mathcal{R}^c) \cup \mathbf{N}(\mathcal{R}^c) \end{array} \tag{5}$$

These sets can be used to evaluate the intersection sets in $\mathbf{I}_{33}$. Intersections between matrices of different types are empty *per definitionem*, so we may reduce for example the interior-interior intersection set between two regions $\mathcal{A}$ and $\mathcal{B}$ to the following equation:

$$\overset{\circ}{\mathcal{A}} \cap \overset{\circ}{\mathcal{B}} \;=\; (\mathbf{C}(\overset{\circ}{\mathcal{A}}) \cap \mathbf{C}(\overset{\circ}{\mathcal{B}})) \;\cup\; (\mathbf{E}(\overset{\circ}{\mathcal{A}}) \cap \mathbf{E}(\overset{\circ}{\mathcal{B}})) \;\cup\; (\mathbf{N}(\overset{\circ}{\mathcal{A}}) \cap \mathbf{N}(\overset{\circ}{\mathcal{B}})) \tag{6}$$

However, we are mainly interested in intersection sets being empty or not, and only less interested in the completeness of an intersection set. Therefore, we now refer to the possible dimensions of the nine intersection sets[5] (Table 3).

Proposition 4.1: If an intersection set is either of dimension 2 or empty, and if the intersection set is not empty, there must exist a (non-empty) set $\mathbf{C}(\mathcal{A}) \cap \mathbf{C}(\mathcal{B})$.

Proposition 4.2: If an intersection set is either of dimension 1 or empty, and if the intersection set is not empty, there must exist a (non-empty) set $\mathbf{E}(\mathcal{A}) \cap \mathbf{E}(\mathcal{B})$.

Proposition 4.3: If an intersection set is either of dimension 0 or empty, and if the intersection set is not empty, there must exist a (non-empty) set $\mathbf{N}(\mathcal{A}) \cap \mathbf{N}(\mathcal{B})$.

All three propositions are self-evident and do not need further proof. Now, following Table 3, Proposition 4.4 is used for deciding about the intersection sets i_{11}, i_{31}, i_{13}, and i_{33}. With Proposition 4.4 we decide for the intersection sets i_{12}, i_{21}, i_{23}, and i_{32}. Only the boundary-boundary intersection is not fixed in the dimension. It may be both, 1D or 0D. That means that Propositions 4.4 and 4.4 are not applicable. Therefore, we need the

Proposition 4.4: If a non-empty boundary-boundary intersection set exists, there must also exist a non-empty set $\mathbf{N}(\partial\mathcal{A}) \cap \mathbf{N}(\partial\mathcal{B})$.

Proof: The boundary is foreground in $\mathbf{E}$ and $\mathbf{N}$ (see (3,4)). Then it follows from hyper-raster consistency that each foreground pixel $e_{i,j}$ is bounded by two foreground pixels $n_{k,l}$ and $n_{m,n}$ (minimum condition for 1D-intersection). On the other hand, if the intersection is 0D, it is evident that $\mathbf{E}(\partial\mathcal{A}) \cap \mathbf{E}(\partial\mathcal{B})$ is empty, so there must exist a non-empty $\mathbf{N}(\partial\mathcal{A}) \cap \mathbf{N}(\partial\mathcal{B})$. □ ■

With these considerations we can now reduce the calculations for the intersection sets of $\mathbf{I}_{33}$ to the overlays given in Table 4. As one consequence we directly gather from that table that there is no further need to build $\mathbf{N}(\overset{\circ}{\mathcal{R}})$ or $\mathbf{N}(\mathcal{R}^c)$.

[5] In Sect. 4.3 we have shown that these dimensions will hold in hyper-raster, too.

Table 4: Operations to calculate the intersection sets of $\mathbf{I}_{33}$ from hyperimage matrices.

	$\mathring{\mathcal{B}}$	$\partial\mathcal{B}$	$\mathcal{B}^c$
$\mathring{\mathcal{A}}$	$\mathbf{C}(\mathring{\mathcal{A}}) \cap \mathbf{C}(\mathring{\mathcal{B}})$	$\mathbf{E}(\mathring{\mathcal{A}}) \cap \mathbf{E}(\partial\mathcal{B})$	$\mathbf{C}(\mathring{\mathcal{A}}) \cap \mathbf{C}(\mathcal{B}^c)$
$\partial\mathcal{A}$	$\mathbf{E}(\partial\mathcal{A}) \cap \mathbf{E}(\mathring{\mathcal{B}})$	$\mathbf{N}(\partial\mathcal{A}) \cap \mathbf{N}(\partial\mathcal{B})$	$\mathbf{E}(\partial\mathcal{A}) \cap \mathbf{E}(\mathcal{B}^c)$
$\mathcal{A}^c$	$\mathbf{C}(\mathcal{A}^c) \cap \mathbf{C}(\mathring{\mathcal{B}})$	$\mathbf{E}(\mathcal{A}^c) \cap \mathbf{E}(\partial\mathcal{B})$	$\mathbf{C}(\mathcal{A}^c) \cap \mathbf{C}(\mathcal{B}^c)$

4.5 Refinements in the Hyper-Raster

For transferring the refinements to the hyper-raster we will use the overlay of extraction matrices more extensively. Several additional measures can be calculated:

- the *dimension* of an intersection set. As in the vector model, this concerns only the boundary-boundary intersection, which can be 1D or 0D (or -1D, in case of $\emptyset$). The dimension is determined by the type of the matrix which contains the intersection set: if $\mathbf{E}(\partial\mathcal{A}) \cap \mathbf{E}(\partial\mathcal{B})$ is not empty, then this set is 1D, and if only $\mathbf{N}(\partial\mathcal{A}) \cap \mathbf{N}(\partial\mathcal{B})$ is not empty, then the set is 0D. The dimensions of the other intersection sets are fixed.
- the *number of separations*. This is done by counting the connected components (Lumia *et al.* 1983, Bässmann and Besslich 1991) in the intersection matrices. The intersection matrices of **C**'s and **E**'s are sufficient for this task, because a junction is at least 1D.
- *component features*. Performing feature extraction yields a list of further parameters, characterizing the single intersection component: the size, the perimeter, the main axes, compactness, the center of gravity, the orientation, and other features. These parameters are no topological invariants (e.g. Bässmann and Besslich 1991).
- the *type* of boundary-boundary intersections (*crossing / touching*). This type follows from contour tracking through both considered **E** matrices.

5 Example

We may be interested in the topological relation between the following regions $\mathcal{A}$ and $\mathcal{B}$ (Fig. 5). Assume, that the two vector sets refer to the same real world object, but it is associated in one GIS map with three boundary points, and in another with four boundary points.

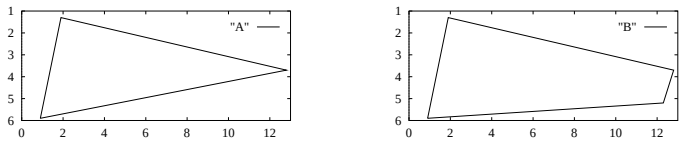

Figure 5: A region in two different vector maps.

The digitization into discrete *hyperimages* (one per vector region) follows Sect. 4.2. The result are three matrices $\mathbf{C}_e$, $\mathbf{E}_e$, and $\mathbf{N}_e$ for each region (Fig. 6). With these matrices we create intersection matrices (Fig. 7) and determine the topological relation between $\mathcal{A}$ ('the region from map A') and $\mathcal{B}$ ('the region from map B').

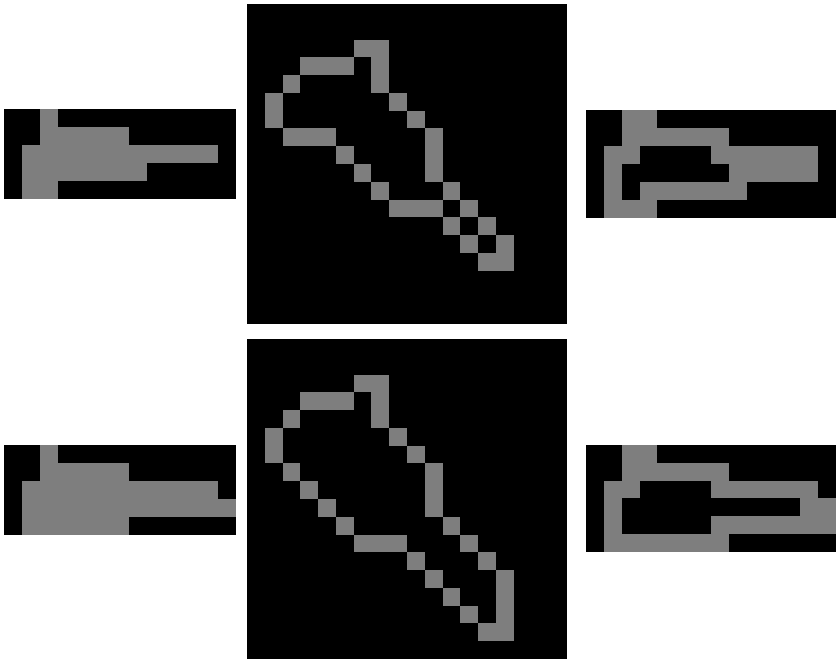

Figure 6: The hyperimage matrices $\mathbf{C}_e(\mathcal{A})$, $\mathbf{E}_e(\mathcal{A})$, and $\mathbf{N}_e(\mathcal{A})$ (top line), $\mathbf{C}_e(\mathcal{B})$, $\mathbf{E}_e(\mathcal{B})$, and $\mathbf{N}_e(\mathcal{B})$ (bottom line). Foreground is bright. We can also see the rotation and scale of $\mathbf{E}$.

From the intersection matrices we can derivate the 9-intersection matrix (the element i_{33} is not evaluated because it is never empty):

$$|\mathbf{I}_{33}| = \begin{pmatrix} 26 & 0 & 0 \\ 10 & 24 & 0 \\ 9 & 12 & - \end{pmatrix} \tag{7}$$

This matrix is equivalent to the topological relation CoveredBy $(\mathcal{A}, \mathcal{B})$ (cf. Table 2). A refined description of the relation will contain:

- Dimension of boundary-boundary intersection: 1D.
- Number of components:

$$\text{no\_components}\,(\mathbf{I}_{33}) = \begin{pmatrix} 1 & 0 & 0 \\ 2 & 2 & 0 \\ 1 & 2 & (1) \end{pmatrix} \tag{8}$$

Further attributes of the components are not evaluated here.

6 Conclusions

We have presented a model and a data structure to realize a topological reasoning between two regions without holes in images within the topology of $\mathbb{R}^2$. Our model overcomes the topological defect of the simple raster model, and is able to compute easily and quickly a detailed description of topological relations. The model is capable of reasoning with objects of other dimensions, and with holes, which has to be demonstrated later.

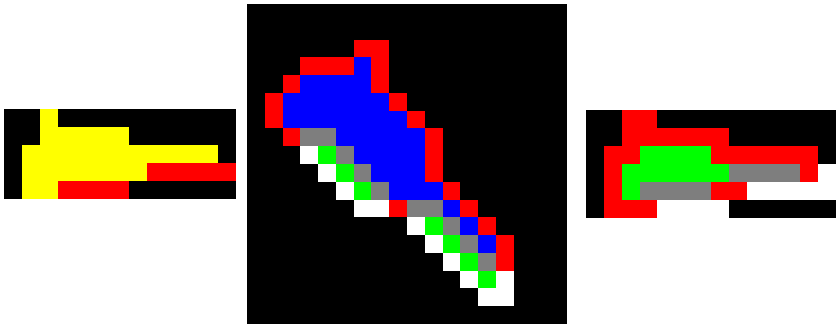

Figure 7: The intersection sets of the **C**-, **E**- and **N**-matrices. The sets are differentiated by gray intensities.

The proposed data structure is intuitively clear, and the adapted size of the reasoning area to the overlap of bounding rectangles speeds up the reasoning enormously. Compared to the complex calculations in $\mathbb{R}^2$, we are in advantage because binary images are discrete and the applied image processing needs no higher computations than comparison and counting. The proposed *hyperimage* structure is well suited for demonstrating intersection sets, but up to now is not optimized for memory and access. Changing the structure is possible in the object-oriented paradigm.

Therefore, we propose to choose the hyper-raster as a general model for topological reasoning in spatial databases and GIS. Some work is required to complete the model for curves and points, and to open the model to the whole world of image processing tasks, e.g. for image segmentation, contour tracking *et cetera*. But the advantages which compensate for this work, are, in particular, explicit elements for edges and vertices, and a discrete computation space.

References

Ballard, Dana H.; Brown, Christopher M. (1982): *Computer Vision*. Prentice Hall, Englewood Cliffs, NJ, 1982.

Bässmann, Henning; Besslich, Philipp (1991): *Bildverarbeitung Ad Oculos*. Springer, Berlin, 1991.

Bennis, K.; David, B.; Morize-Quilio, I.; Thevenin, J. M.; Viemont, Y. (1991): GeoGraph: A Topological Storage Model for Extensible GIS. In: *Auto-Carto 10*, pages 349–367, Baltimore, 1991. ACSM — ASPRS.

Bieri, Hanspeter; Metz, Igor (1991): A Bintree Representation of Generalized Binary Digital Images. In: Eckhardt, Ulrich; Hübler, Albrecht; Nagel, Werner; Werner, Günther (Eds.), *Geometrical Problems of Image Processing*, pages 72–77, Berlin, 1991. Akademie Verlag.

Clementini, Eliseo; Di Felice, Paolino (1994): A Comparison of Methods for Representing Topological Relationships. *Information Sciences 80*, pages 1–30, 1994.

Clementini, Eliseo; Di Felice, Paolino; van Oosterom, Peter (1993): A Small Set of Formal Topological Relationships Suitable for End-User Interaction. In: Abel, D.; Ooi, B. (Eds.), *Advances in Spatial Databases*, pages 277–295, New York, 1993. 3rd Symposium on Large Spatial Databases SSD '93, Springer LNCS 692.

Egenhofer, Max J.; Franzosa, Robert D. (1991): Point-set topological spatial relations. *Int. Journal of Geographical Information Systems*, 5(2):161–174, 1991.

Egenhofer, Max J.; Herring, John R. (1991): Categorizing Binary Topological Relationships Between Regions, Lines, and Points in Geographic Databases. Technical report, Department of Surveying Engineering, University of Maine, Orono, ME, 1991.

Egenhofer, Max; Sharma, Jayant (1993): Topological Relations Between Regions in R^2 and Z^2. In: Abel, D.; Ooi, B. (Eds.), *Advances in Spatial Databases*, pages 316–336, New York, 1993. 3rd Symposium on Large Spatial Databases SSD '93, Springer LNCS 692.

Egenhofer, Max J.; Clementini, Eliseo; di Felice, Paolino (1994): Topological relations between regions with holes. *International Journal of Geographical Information Systems*, 8(2):129–142, 1994.

Egenhofer, Max J.; Clementini, Eliseo; Di Felice, Paolino (1994): Evaluating Inconsistencies among Multiple Representations. In: Waugh, Thomas C.; Healey, Richard G. (Eds.), *Advances in GIS Research*, pages 901–919, Edinburgh, 1994. Proc. 6th Int. Symp. on Spatial Data Handling.

Egenhofer, Max J. (1993): A Model for Detailed Binary Topological Relationships. *Geomatica*, 47(3 & 4):261–273, 1993.

Hernández, Daniel (1994): *Qualitative Representation of Spatial Knowledge.* LNAI 804. Springer, Berlin, 1994.

Herring, J.R. (1987): TIGRIS: Topologically Integrated Geographic Information System. In: *Auto-Carto 8*, pages 282–291, Baltimore, 1987. ACSM — ASPRS.

Jänich, Klaus (1994): *Topologie.* Springer, Berlin, 4. edition, 1994.

Kong, T. Y.; Rosenfeld, A. (1989): Digital Topology: Introduction and Survey. *CVGIP 48*, pages 357–393, 1989.

Kovalevski, V. A. (1989): Finite topology as applied to image analysis. *CVGIP 46*, pages 141–161, 1989.

Kropatsch, Walter G. (1985): A pyramid that grows by powers of 2. *Pattern Recognition Letters*, 3:315–322, 1985.

Kropatsch, Walter (1986): Grauwert- und Kurvenpyramide, das ideale Paar. In: Hartmann, G. (Ed.), *Mustererkennung 1986*, pages 79–83, Berlin, 1986. 8. DAGM-Symposium, Springer.

Latecki, Longin; Eckhardt, Ulrich; Rosenfeld, Azriel (1995): Well-Composed Sets. *Computer Vision and Image Understanding*, 61(1):70–83, 1995.

Latecki, Longin (1992): *Digitale und Allgemeine Topologie in der bildhaften Wissensrepräsentation*, Band 9 der Reihe DISKI. infix, St. Augustin, 1992.

Lumia, Ronald; Shapiro, Linda; Zuniga, Oscar (1983): A New Connected Components Algorithm for Virtual Memory Computers. *Computer Vision, Graphics, and Image Processing*, pages 287–300, 1983.

Molenaar, Martien; Kufoniyi, O.; Bouloucos, T. (1994): Modelling Topologic Relationships in Vector Maps. In: Waugh, Thomas C.; Healey, Richard G. (Eds.), *Advances in GIS Research*, pages 112–126, Edinburgh, 1994. Proc. 6th Int. Symp. on Spatial Data Handling.

Pigot, Simon (1991): Topological Models for 3D Spatial Information Systems. In: Mark, David M.; White, Denis (Eds.), *Auto-Carto 10*, pages 368–392, Baltimore, 1991. ACSM-ASPRS.

Pilouk, Morakot; Tempfli, Klaus; Molenaar, Martien (1994): A Tetrahedron-based 3D Vector Data Model for Geoinformation. In: Molenaar, Martien; de Hoop, Sylvia (Eds.), *Advanced Geographic Data Modelling*, pages 129–140, Delft, 1994. Netherlands Geodetic Commission.